ELSEVIER

Journal of Molecular Catalysis A: Chemical 169 (2001) 247–257

JOURNAL OF MOLECULAR CATALYSIS A: CHEMICAL

www.elsevier.com/locate/molcata

Anionic platinum carbonyls in zeolites: effect of Si/Al ratio and of zeolitic structure

Jana Nováková*

J. Heyrovský Institute of Physical Chemistry, Academy of Sciences of the Czech Republic, Dolejškova 3, 182 23 Prague 8, Czech Republic

Received 13 September 2000; received in revised form 7 November 2000; accepted 5 December 2000

Abstract

Ship-in-bottle synthesis of anionic platinum carbonyls (Chini complexes) was studied in zeolites of various Si/Al ratio and types — NaLSX, NaX, NaY, dealuminated Y, NaEMT, NaM, NaBEA and MCM-41. The effect of decationation of Y zeolites was also examined. The increasing Si/Al ratio led to the increase of Pt nuclearity, the decationation of Y zeolite did not affect the final carbonyl formed. Recarbonylation of platinum after removal of carbonyl ligands by mild oxidation resulted in anionic carbonyl identical with the primary complex, while some changes were found in samples recarbonylated after decomposition of primary carbonyls via mild heating in vacuum. The carbonylation process was examined in situ by FTIR spectroscopy; the carbonyl complexes were decomposed by programmed heating with mass spectroscopic analysis of gases released.

Keywords: Anionic platinum carbonyls; Effect of various zeolite types; Si/Al between 1 and 54

1. Introduction

Anionic platinum carbonyls (Chini complexes) $[Pt_3(C–O)_3(\mu–CO)_3]_n^{2-}$ have been easily synthesised in solutions as well as anchored on various supports (e.g. [1,2]). They can also be prepared in cavities of microporous zeolites (with $n = 2–3$ without local damage of the zeolite structure) by the so-called 'ship-in-bottle' synthesis using carbonylation of Pt cations in the presence of water, i.e. by water gas shift (WGS) reaction. The charge balancing species in microporous zeolites are either NH_4^+ or H^+ ions. Pt Chini complexes with $n = 5–6$ were synthesised in silicalites from H_2PtCl_6 via intermediate formation of Pt carbonyl chlorides [2,3]. The charge compensating role is played here by organic cations. In addition, mesoporous silica with large pore volume can be used for introduction of ex situ synthesised Chini complexes again with organic charge-compensating cations [4].

The effect of various alkali cations in X and Y zeolites was reported in our previous papers [5,6]. It appeared that the increasing electropositivity (increased basicity of zeolitic oxygens) and radius of the alkali cation result in an increased rate of carbonylation. It was also shown that zeolitic water accelerates the carbonylation and affects positions of the IR CO bands [7] in NaX zeolites. Low platinum nuclearity can be conserved via mild oxidation of Chini complexes [8]. The present contribution concerns a comparison of Pt Chini complexes prepared by 'ship-in-bottle' synthesis in sodium forms of faujasites LSX, X, Y, dealuminated Y, EMT, and in NaM, NaBEA and MCM-41. Y zeolites with various extent of decationation are also included in this study. The recarbonylation of PtNaY

* Tel.: +4202-66053605; fax: +4202-8582307.
E-mail address: novakova@jh-inst.cas.cz (J. Nováková).

1381-1169/01/$ – see front matter
PII: S1381-1169(00)00567-7

after the removal of CO ligands by mild oxidation is compared with the recarbonylation after heat treatment in vacuum.

The accessible cages of LSX, X and Y are comparable, dealuminated Y [9] is characterised by a very low loss of crystallinity; these samples differ in Si/Al ratios (1–6.9). Diameter of the large cavity in EMT zeolite exceeds slightly that of faujasites (approximately 1.4 nm > 1.2 nm [10]); the Si/Al ratio (3.6) is higher than that in NaX and NaY, and matches the Si/Al range of the dealuminated Y zeolites. Mordenite, BEA and MCM-41 exhibit substantially higher Si/Al ratio and different structures. NaM possesses main channels of 0.67 nm × 0.7 nm openings (12 oxygen rings) and pockets (0.39 nm × 0.47 nm separated by 0.28 restrictions), as well as eight oxygen rings [11]. The parent Pt tetrammine complex cannot penetrate into the latter channels, and thus NaM behaves in synthesis of Pt Chini complexes virtually as a monodimensional host. NaBEA is a three-dimensional zeolite with three mutually intersecting 12 ring channels, two linear (0.57 nm × 0.75 nm) and one tortuous (0.56 nm × 0.65 nm) [12]. MCM-41 is characterised by wide linear parallel pores; a sample with pores of 3.2 nm diameter was kindly given by Dr. Zukal [13].

The formation and properties of Pt Chini complexes should thus be affected by:

1. the internal volume in zeolites in which the ship-in-bottle synthesis is performed;
2. the basicity of zeolitic oxygens in different zeolite types;
3. by various extent of decationation in Y zeolite.

2. Experimental

2.1. Parent zeolites

NaX (Si/Al = 1.25, Serva Int.), NaY (Si/Al = 2.5, VURUP, Slovakia), NaLSX (Si/Al = 1, sample described in [14]), and NaEMT (sample Si/Al = 3.6, for details see [10]). To increase the Si/Al ratio in faujasites, NaY was also dealuminated using $SiCl_4$ followed by extraction of the extralattice aluminium by NaOH; the dealuminated sample exhibits Si/Al ratio = 6.9. Sodium in Y and X zeolites was also ion exchanged for NH_4^+ using 0.5 M solution of NH_4Cl. The exchange level was 0.5 for NaX (this sample was used only for calibration, not for carbonylation), 0.2, 0.3 and 0.7 for NaY. NaM with Si/Al = 10.8 and NH_4BEA with Si/Al = 13.5 were supplied by ZEOLYST Int.; NH_4^+ of the latter sample was exchanged for sodium. MCM-41 with Si/Al = 54 was used [13].

2.2. Pt incorporation

Sodium of the samples was partially ion exchanged for $[Pt(NH_3)_4]Cl_2$ to give 3 wt.% of Pt (at 25°C for 2 days, then washed and dried at the same temperature). In addition, NaX zeolite with higher Pt content (10.5 and 17.5 wt.%) was also prepared. The Pt loading was checked by AAS analysis of the solution and of the dissolved zeolites after the ion exchange. NaM, NaBEA and MCM-41 were also either ion exchanged with Pt tetrammine ions, or impregnated according to Yamamoto et al. and Sasaki et al. [2,3] by Et_4NCl and H_2PtCl_6; the impregnated samples contained 5 wt.% of Pt.

2.3. Carbonylation procedure

Ion exchanged zeolites were evacuated for 30 min at 25°C and then carbonylated by 600 mbar of CO at 90°C for 24–48 h in situ in the infrared cell (a MX1E Nicolet FTIR instrument, resolution of 2 cm^{-1}, self-supported pellets of 7 mg cm^{-2}, spectra measured at room temperature, samples heated after lifting to the upper part of the apparatus). The final carbonylation time was given by the disappearance of the deformation vibrations of N–H in Pt ammines (1380 cm^{-1}), and by no further increase of N–H bands in NH_4^+ (at about 1470 cm^{-1}) and of stretching CO vibrations (around 1800 and 2040 cm^{-1}). The carbonylation of impregnated samples (NaM, NaBEA and MCM-41) was carried out by the procedure described in [2,3], i.e. by treatment with 250 mbar of CO for 3 h, then with 250 mbar of CO + 20 mbar of H_2O for 12 h. Both these procedure were carried out at 50°C.

2.4. TPD

The temperature programmed decomposition (TPD) in vacuum of parent tetrammine ions in zeolites and of Chini complexes created via carbonylation of these complexes was performed using 5 mg of the samples; heating rate was 5°C min^{-1} (60–420°C).

Gases released were led directly into the vacuum system of a Balzers 420 quadrupole mass spectrometer. Ions with $m/z = 16$ represent the ammonia released; these ions are only negligibly affected by fragments of water. CO released during the TPD of carbonyls was also registered (ion 28, accompanied by the fragment ion 12; this fragment ion is important to distinguish molecular ion of CO from that of N_2 to which belongs the fragment ion 14).

3. Results

3.1. Pt Chini complexes in zeolites, FTIR spectra

The IR spectra of carbonylated platinum tetrammine ions in NaLSX (top spectrum), NaX (a–c), NaY (1), $NaNH_4Y$ (2–4) shown in Fig. 1A were registered after carbonylation of Pt tetrammine ions in partially hydrated zeolites (ca. 50% of zeolitic water was removed by pre-treatment in vacuum at 25°C). It follows that Pt anionic carbonyls in NaLSX and NaX exhibit the same CO bands — the bridge ones at 1783 cm^{-1} and the linearly bonded CO at 2049–2053 cm^{-1}. The shoulder at about 1800 cm^{-1} belongs to the Pt Chini complex in the dehydrated sample [7]. The wavenumbers of bridge-bonded CO in NaY exhibit, in addition to the band at 1783 cm^{-1}, also a rather strong band at 1818 cm^{-1}, the on-top bonded CO ligands vibrate at 2053 cm^{-1}. The NH_4^+ bands are shifted from 1470 to 1457 cm^{-1} with the increasing Si/Al ratio. The band at 1595 cm^{-1} found in more Pt enriched NaX (spectra b and c) could be assigned to asymmetric N–H vibrations (present also in $NaNH_4Y$, spectra 2–4).

The Chini complexes in samples with higher Si/Al ratio are shown in Fig. 1B for NaY_{deal}, NaEMT and MCM-41. The on-top bonded CO bands are shifted to higher wavenumbers compared with those in the preceding samples (2050 → 2065–2080 cm^{-1}); the bridge-bonded CO also lie at higher wavenumbers

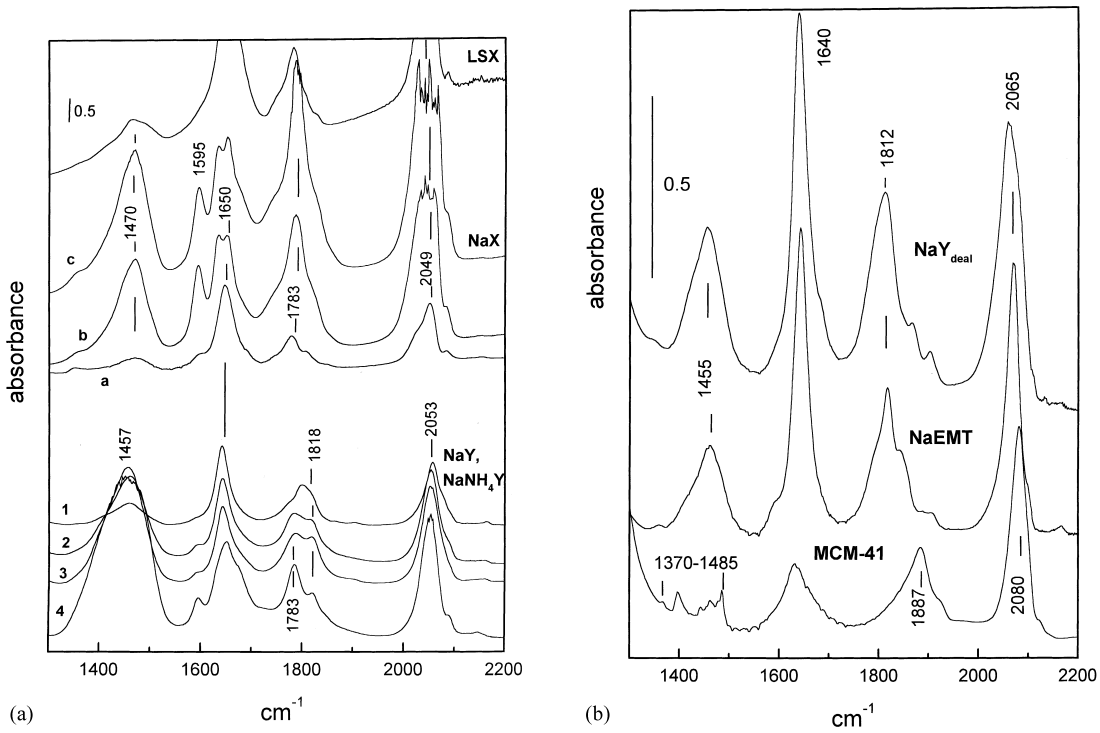

Fig. 1. IR spectra of Pt Chini complexes in various zeolites: (A) 1–4 in NaY, $Na_{0.8}(NH_4)_{0.2}Y$, $Na_{0.7}(NH_4)_{0.3}Y$ and $Na_{0.3}(NH_4)_{0.7}Y$, respectively (3 wt.% of Pt), a–c in NaX with 3, 10.5 and 17.5 wt.% of Pt, respectively, top spectrum in NaLSX (3 wt.% of Pt); (B) in NaEMT and Y_{deal} (both with 3 wt.% of Pt) and in MCM-41 (5 wt.% of Pt).

Table 1
Integrated values of bridge and on-top bonded CO IR bands[a]

Initial sample	Si/Al	Area *A*, CO bridge, (arbitrory unit)	Area *B*, CO on-top (arbitrory unit)	*B*/*A*
PtNaLSX-3	1.0	200	324	1.6
PtNaX-3	1.25	182	319	1.7
PtNaX-10.5	1.25	610	897	1.5
PtNaX-17.5	1.25	790	1000	1.3
PtNaY-3	2.5	162	195	1.2
$PtNa_{0.8}Y$-3	2.5	186	271	1.5
$PtNa_{0.7}Y$-3	2.5	210	268	1.3
$PtNa_{0.3}Y$-3	2.5	163	301	1.8
$PtNaY_{deal}$-3	6.9	188	231	1.2
PtNaEMT-3	3.6	200	243	1.2
MCM-41-5	54	74	122	1.6

[a] Numbers following the dash in the first column give the wt.% of platinum. Values related to the area of the on-top CO band in PtNaX-17.5 (1000).

(1783 → 1812–1887 cm^{-1}). The former two samples were carbonylated in the same way as those in Fig. 1A, spectrum of MCM-41 was obtained by carbonylation of the sample impregnated with Et_4NCl and H_2PtCl_6. Virtually, the same spectra as in MCM-41 were obtained for Pt carbonyls in NaM and NaBEA (not shown here).

The integrated values of the CO bands (related to the area of the band of linearly bonded CO in PtNaX with 17.5 wt.% of Pt-1000) and their ratio are given in Table 1. The intensity ratio of on-top to bridge bonded CO is of about 1.5. Colour of all X zeolites

Table 2
Integrated values of NH_3 IR bands in Pt tetrammines before carbonylation and in NH_4^+ after carbonylation[a]

Sample	N–H prior to carbonylation, *A*	N–H after carbonylation, *B*	*B*/*A*
PtNaLSX-3	106	124	1.2
PtNaX-3	130	154	1.2
	156 (120°C)	181	1.2
	124	117	0.9
	136	124	0.9
	132	154	1.2
PtNaX-10.5	393	540	1.4
PtNaX-17.5	505	600	1.2
PtNaY-3	61	107	1.7
$PtNa_{0.8}Y$-3[b]	292	409	1.4
$PtNa_{0.7}Y$-3[b]	423	571	1.3
$PtNa_{0.3}Y$-3[b]	749	907	1.2
$PtNaY_{deal}$-3	73.6	114	1.5
PtNaEMT-3	83	126	1.5
$Na_{0.8}Y$	279	–	–
$Na_{0.7}Y$	402	–	–
$Na_{0.3}Y$	1000	–	–
$Na_{0.65}X$	303 (100°C)	–	–

[a] Areas calculated from following vibrations (cm^{-1}); $N–H_{ammine}$: 1350–1380 cm^{-1}; $N–H_{ammonia}$: 1460 cm^{-1}; numbers following the dash in the first column give the wt.% of platinum.
[b] For the ammines in $PtNa(NH_4)Y$ zeolites the whole range 1350–1460 was integrated.

Table 3
Ammonia released during the TPD of Pt tetrammine from zeolites (*A*) and from zeolites with Pt carbonyl (*B*) complexes[a]

Sample	$[Pt(NH_3)_4]^{2+} \rightarrow NH_3$	$NH_4^+ \rightarrow NH_3 + H^+$
	A (μmol)	*B* (μmol)
PtNaLSX-3	3.7 (4.8)	1.4 (1.8)
PtNaX-3	3.0 (3.9)	1.5 (2)
PtNaX-10.5	11.0 (4.1)	4.1 (1.5)
PtNaX-17.5	14.9 (3.3)	5.3 (1.2)
PtNaY-3	3.6 (4.7)	2.4 (2.1)
$PtNa_{80}Y$-3	7.9	5.0
$PtNa_{70}Y$-3	8.3	10.45
$PtNa_{30}Y$-3	14.8	14.8
$PtNaY_{deal}$-3	3.4 (3.9)	2.2 (2.8)
PtNaEMT-3	3.3 (4.2)	1.0 (1.3)
$Na_{35}X$	–	10.9
$Na_{80}Y$	–	4.0
$Na_{70}Y$	–	5.3
$Na_{30}Y$	–	12.2

[a] Sample weight 0.48–6.2 mg, in table normalised to 5 mg; values in parentheses are related to the amount of platinum; not calculated for decationated Y.

after carbonylation was orange–brown, brownish in Y, nicely violet in EMT and greyish in NaY_{deal}. Colour of carbonylated Pt complexes in MCM-41, NaM and NaBEA was yellow–green.

The integrated values of N–H deformation vibrations in Pt tetrammine ions prior to carbonylation (1380 cm^{-1}, not shown here) and in NH_4^+ (1450–1470 cm^{-1}, Fig. 1A and B) after carbonylation and their ratios are given in Table 2. This ratio is of about 1.4 in average, the values are rather scattered.

3.2. TPD of carbonyls, release of ammonia

The ammonia released from samples prepared by carbonylation of Pt tetrammine ions is compared with ammonia released during the decomposition of the

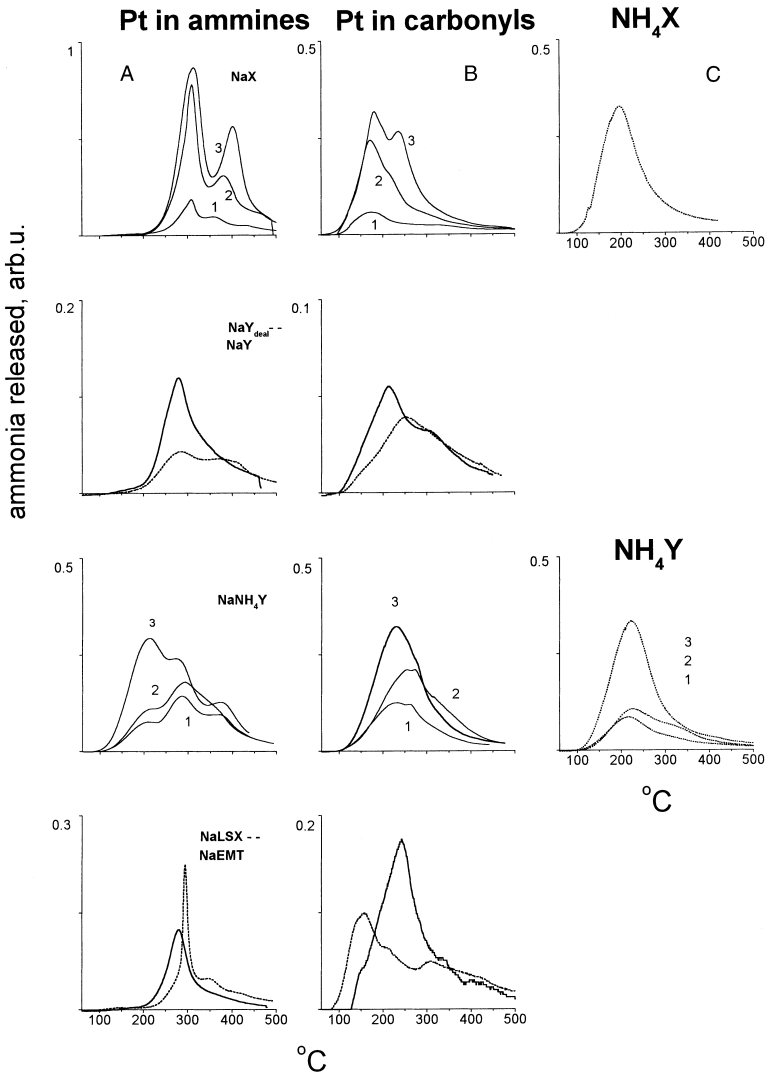

Fig. 2. TPD of Pt tetrammines and carbonyls, release of ammonia: (A) ammonia released from Pt tetrammines, from top to bottom, in NaX: curves 1–3 with 3, 10.5 and 17.5 wt.% of Pt, respectively; in NaY_{deal} dashed, in NaY solid (3 wt.% of Pt); 1–3 in $Na_{0.8}(NH_4)_{0.2}Y$, $Na_{0.7}(NH_4)_{0.3}Y$ and $Na_{0.3}(NH_4)_{0.7}Y$, respectively (3 wt.% of Pt); in NaEMT solid, in NaLSX dashed (3 wt.% of Pt); (B) ammonia released from Pt carbonyls, denotation the same as in section A; (c) ammonia released from NH_4NaX and $NaNH_4Y$, zeolites prior to Pt ammine incorporation.

parent tetrammine ions in Fig. 2. It can be seen that ammonia from the ammine ions (section A) begins to desorb irrespective of the host zeolite from 200°C, from $NaNH_4Y$ and $NaNH_4X$ without platinum above 100°C (section C, the desorption from Pt tetrammine ions in $NaNH_4Y$ is shifted towards this temperature due to the desorption of NH_4^+ ions). The maxima of desorbed ammonia from the carbonylated samples (section B) are shifted to higher temperatures with the increasing Si/Al ratio: NaLSX < NaX < NaY < NaY deal ≅ NaEMT (155, 175, 225, 240–250°C, respectively). This agrees with the assumption that the NH_4^+ ions in carbonylated samples are of similar nature as those in ammonia forms of these zeolites without platinum, and that the above sequence reflects the increased acidity of the OH groups. Moreover, the ammonia maximum of $NaNH_4X$ and $NaNH_4Y$ lies at the same temperature as that from carbonyls, which again shows that the NH_4^+ ions formed during carbonylation balance the zeolitic charge similarly as these ions in ammonium forms of zeolites.

The amount of evolved ammonia (in μmol, calibrated by ammonia release from $Na_{0.3}(NH_4)_{0.7}Y$ without platinum) is listed in Table 3. The values in parantheses represent the ratio of evolved ammonia to the amount of platinum; this ratio for ammines (4) is higher than that for carbonyls.

3.3. CO released during TPD of carbonyls

Fig. 3A shows the release of carbon monoxide during the TPD of carbonyls from X, Y, LSX, Y_{deal} and EMT. First, maxima appear between 120 and 175°C irrespective of the zeolitic host, substantially lower maxima are found at about 350°C. Only LSX

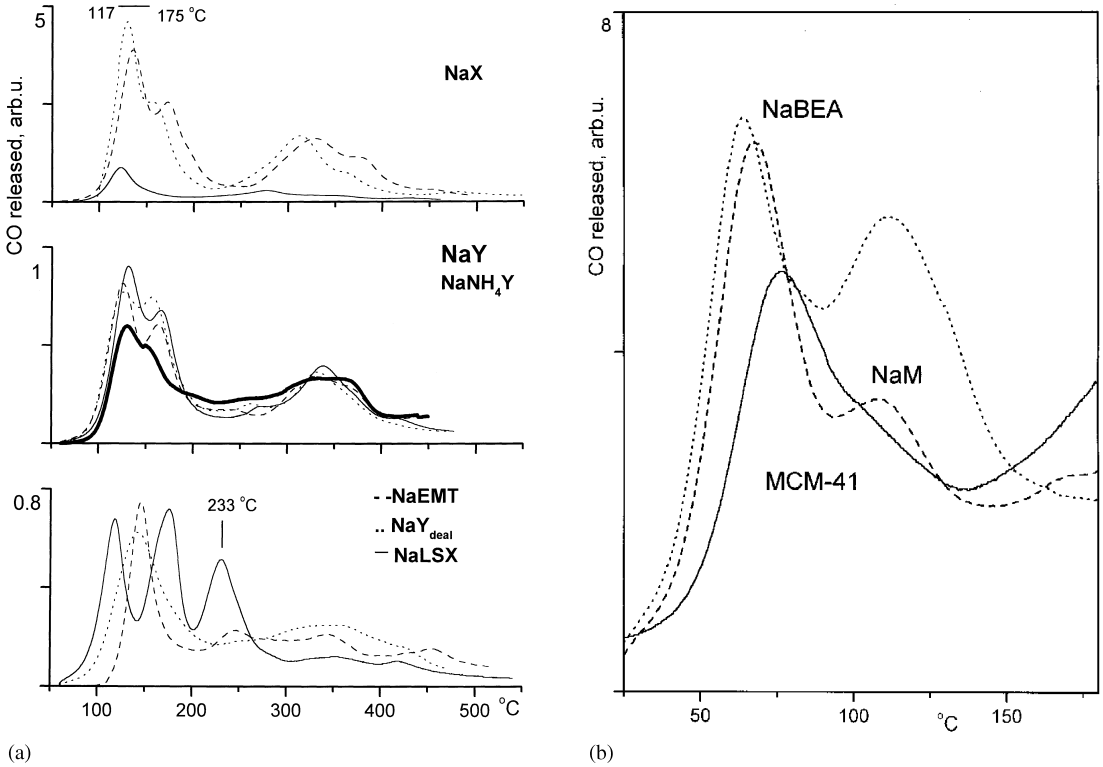

Fig. 3. TPD of Pt carbonyls, release of CO: (A) top part: solid, dashed and dotted from NaX with 3, 10.5 and 17.5 wt.% of Pt, respectively, middle part: solid bold, dashed, solid fine and dotted from NaY, $Na_{0.8}(NH_4)_{0.2}Y$, $Na_{0.7}(NH_4)_{0.3}Y$ and $Na_{0.3}(NH_4)_{0.7}Y$, respectively (3 wt.% of Pt), bottom part: solid, dotted and dashed from NaLSX, Y_{deal} and NaEMT, respectively (3 wt.% of Pt); (B) from NaM, NaBEA, and MCM-41 (5 wt.% of Pt).

exhibits three distinct maxima, two former in the same low-temperature region as for the other zeolites, and one at about 230°C. In Fig. 3B the release of CO during the TPD of carbonyls in NaM, NaBEA and MCM-41 is displayed. It follows that the first maxima appear below 100°C. The TPD curves are shown only to the temperature of 180°C, because at higher temperatures the decomposition of Et_4N occurs.

3.4. Recarbonylation of Y zeolites after removal of the CO ligands by mild oxidation and/or by vacuum at mild temperature, FTIR spectra

Fig. 4 shows the IR spectra of Pt Chini complexes in NaY and $NaNH_4Y$ formed by carbonylation of Pt tetrammines (solid spectra), by the recarbonylation of oxidised carbonyls (oxidised at 90°C by 600 mbar of O_2 for 2 h, dashed spectra), and by recarbonylation after vacuum decomposition of the carbonyl (decomposed at 150°C for 2 h, dotted spectra). The recarbonylations were carried out at the same temperature and CO pressure as the carbonylation of Pt tetrammine. It follows that the recarbonylation after mild oxidation does not change positions of the maxima neither the shape of the CO bands, the intensity is only a little lower than in the primary carbonyls. However, the recarbonylation after vacuum heat treatment substantially diminishes the band of NH_4^+ vibrations (at 1460 cm^{-1}) and shifts upwards both the maxima of the on-top and bridge bonded CO. The colour of the samples recarbonylated after vacuum decomposition is rather greyish than brownish. The IR spectra of Pt Chini complexes in NaY and $NaNH_4Y$ exhibit the same features after the carbonylation of Pt tetrammines and after both recabonylations irrespective of the decationation degree.

IR spectra in the 3200–3800 cm^{-1} region are shown in the left-hand side of Fig. 5 for Pt carbonyl in NaY: from bottom to top — prior to carbonylation, after primary carbonylation, after recarbonylation of the

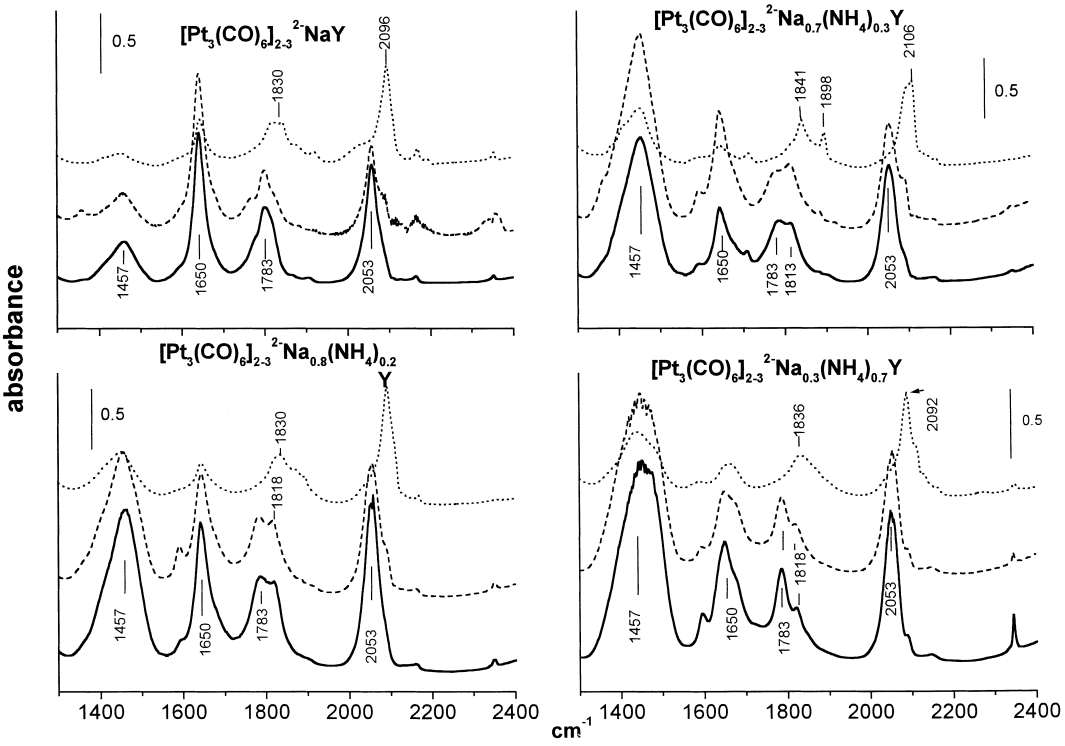

Fig. 4. IR spectra of Pt carbonyls in NaY and $NaNH_4Y$ and spectra of recarbonylated samples. Solid spectra — carbonylated Pt ammines, dashed spectra — samples recarbonylated after removal of CO ligands by mild oxidation, dotted spectra — samples recarbonylated after removal of CO ligands in vacuum at 150°C.

oxidised carbonyl (dashed) and after recarbonylation post vacuum decomposition of the carbonyl (dotted). The former three spectra exhibit bands at 3250, 3550–3420 and 3694 cm^{-1}, the dotted spectrum only the bands corresponding to OH groups in large and small cavities (3646 and 3550 cm^{-1}, respectively). The same changes can be seen in all $PtNaNH_4Y$ samples, only the intensities of the spectra of HF OH groups and LF OH, which are developed in recarbonylation after vacuum treatment of the Pt carbonyl, increase with decreasing content of Na^+ (spectra in the right-hand side of Fig. 5). The IR band at 3694 cm^{-1} most probably belongs to Pt–OH vibrations: this band is not present in $NaNH_4X$ and $NaNH_4Y$ zeolites without platinum, its intensity decreases with increasing dehydration of the samples. In addition, it is also found after calcination of Pt tetrammine ions to Pt^{2+}, i.e. in samples without any nitrogen compounds. According to literature, this band can be assigned to water interacting with M^{2+} [15], in our case with Pt^{2+}.

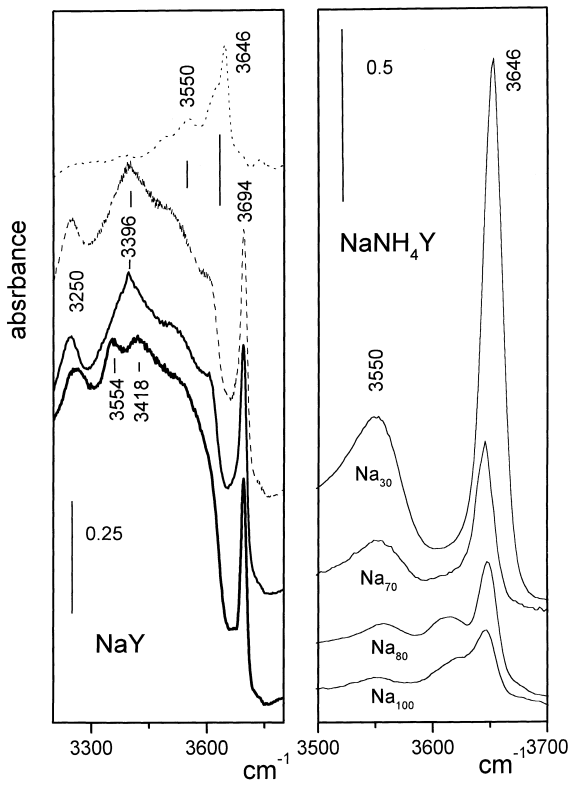

Fig. 5. IR spectra of the stretching N–H and O–H vibrations, effect of recarbonylation. Left-hand side, NaY, from bottom to top: parent Pt tetrammine, carbonylated Pt tetrammine, recarbonylated sample after removal of CO ligands by mild oxidation (dashed spectrum), recarbonylated sample after removal of CO ligands in vacuum at 150°C (dotted spectrum). Right-hand side, OH groups in recarbonylated sample after removal of CO ligands in vacuum at 150°C from NaY, $Na_{80}(NH_4)_{20}Y$, $Na_{70}(NH_4)_{30}Y$ and $Na_{30}(NH_4)_{70}Y$.

4. Discussion

4.1. FTIR spectra of primary carbonyls

Data in Table 1 and IR spectra in Fig. 1A show that carbonyls in LSX and NaX zeolites exhibit the linearly bonded as well as bridge bonded CO at the same wavenumbers, in NaX irrespective of platinum loading. In line with previous results [7] these Chini complexes represent double stacked complex of Pt nuclearity equal to 6 ($[Pt_3(CO)_6]_2^{2-}$).

The positions of both CO ligands in NaY are not affected by the exchange of sodium for NH_4^+, but, compared with those in NaX and NaLSX zeolites, the on-top CO and a part of bridge bonded CO ligands are shifted to a little higher wavenumbers (Fig. 1A, spectra1–4). Previous UV–VIS spectra of carbonyls in Y zeolites point to a mixture of nuclearities ≥ 2 [5,6], their colour is between light-brown, brownish. Shifts of the IR wavenumbers of CO ligands to higher values were found to correspond with the increasing nuclearity of Pt anionic complexes (e.g. [2] and references in [5]), which is in line with the above results. It is possible to assume that the higher basicity of zeolitic oxygens in LSX and X zeolites prefers formation of hexanuclear Pt anionic carbonyls and that the formation of mixed hexa and ennea ($n = 9$) nuclear complexes in NaY is due to the decreased basicity of its oxygens. However, even lower basicity of partially decationated Y zeolites does not affect positions of the CO IR bands (Fig. 1A).

Further increase of the Si/Al ratio in dealuminated Y and NaEMT (Fig. 1B) results in more pronounced shifts of both bridge- and on-top bonded CO ligands. The virtually enneanuclear — triple stacked Pt anionic complex was recently ascribed to the violet carbonyl in NaEMT [10]. It is tempting to assume that the same complex is formed in dealuminated Y because of very similar positions of both CO bands, but the colour of this complex is more similar to that in Y than in EMT

zeolite. The formation of the triple-stacked violet carbonyl complex in NaEMT was related to special spatial arrangement of the zeolite [10], so that not only the Si/Al ratio of the zeolites (and similar dimensions of the cavities) determine the dimensions of the anionic Pt carbonyls. The cavities of X, Y and EMT zeolites allow to incorporate triple stacked Pt carbonyls, as follows from the Pt–Pt, Pt–CO and C–O distances (e.g. [16,17]).

Nuclearity of the Pt carbonyl in MCM-41 can be related to $n = 4$–6 (i.e. Pt nuclearity $n \geq 12$, $[Pt_3(CO)_6]_{4–6}{}^{2-}$), due to the position of CO bands and yellow–green colour. These features were reported in [2,3] and were assigned to the above nuclearity. This assignment was based on the EXAFS, IR and UV–VIS spectra. Pt carbonyls in MCM-41, NaM and NaBEA were obtained only by the carbonylation of samples coimpregnated with Et_4NCl. The carbonylation of ion exchanged $[Pt(NH_3)_4]^{2+}$ in NaM, NaBEA and MCM-41 was unsuccessful. The latter samples were greyish and exhibited only linearly bonded CO at 2067 (NaM) or 2090 cm^{-1} (NaBEA and MCM-41). High Si/Al ratio of these samples resulting in small amount of charge-compensating alkali cations and low basicity of zeolitic oxygens clearly cannot stabilise the anionic carbonyl complex. The incorporation of the relatively large Pt anionic complex in pores of these zeolites would be possible only in MCM-41, in both NaBEA and NaM the location on the outer surface seems to be more probable. The location inside the pore system of MCM-41 can be, due to the channel size, similar to the outer surface of the former two samples.

The ratios of integrated on-top to bridged CO were found to be within 1.2–1.8 irrespective of the carrier (Table 1). This ratio should be 1, the higher value points to higher absorption coefficient of the on-top bonded CO; the independence on the host sample show that in all cases the carbonyls contain one on-top and one bridge bonded ligand per one Pt atom.

4.2. CO released during TPD of carbonyls

Fig. 3A shows that the vacuum decomposition of Pt carbonyls prepared by carbonylation of Pt tetrammine ions starts near to 100°C. The Pt nuclearity is, at least partially, preserved to 150°C, as the recarbonylation yields again Pt carbonyls. This is shown for NaY and $NaNH_4Y$ in Fig. 4.

Maximum of CO from carbonyls in NaM, NaBEA and MCM-41 is released in the same temperature interval as that of carbonyls prepared from Pt tetrammine ions, however, the carbonyls cannot be reconstructed even after the 'low' temperature decomposition of primary CO complexes, neither when using mild oxidation nor vacuum mild heat treatment.

4.3. Ammonia released during TPD and IR N–H deformation vibrations

The vacuum decomposition of Pt tetrammines in zeolites according to Exner et al. [18,19] results in autoreduction of Pt^{2+} to Pt^0, so that only 3/4 of the ammonia ligands are released as NH_3.

$$\{[Pt(NH_3)_4]^{2+}\} \rightarrow \{Pt^0\} + \{2H^+\} + 3NH_3 + \tfrac{1}{2}N_2 + \tfrac{1}{2}H_2 \quad (1)$$

It was shown [20] that better pumping of the released gases decreases the extent of autoreduction and some Pt^{2+} ions are also formed.

$$\{[Pt(NH_3)_4]^{2+}\} \rightarrow \{Pt^{2+}\} + 4NH_3 \quad (2)$$

where braces are used to express anchoring in zeolites. This means that the amount of ammonia released from one Pt tetrammine complex should be between 3 and 4 ($NH_3/Pt = 3$–4). Data in Table 3 show that the evolved ammonia corresponds better with the stoichiometry (Eq. (2)).

When the anionic Pt carbonyl $[Pt_3(CO)_6]_n{}^{2-}$ is synthesised in the cavities of NaX zeolite, formation of the 'double stacked' complex ($n = 2$) is expected to proceed via the route (Eq. (3)).

$$\{6[Pt(NH_3)_4]^{2+}\} + 19CO + 7H_2O \rightarrow \{[Pt_3(CO)_6]_2{}^{2-}\} + \{14NH_4{}^+\} + 10NH_3 + 7CO_2 \quad (3)$$

The decomposition of the carbonylated sample then gives $NH_3/Pt = 14/6 = 2.3$. Values in Table 3 lie within the range 1.2–3.1 (except the more decationised NaY); these scattered values cannot be used for the evaluation of the nuclearity of platinum in the anionic carbonyls: the changes in NH_3/Pt ratios due to the increasing nuclearity are too low, e.g. the formation of anionic carbonyl with $n = 3$ (e.g. in EMT zeolite) can

be described by Eq. (4), which gives the $NH_3/Pt = 20/9 = 2.2$.

$$\{9[Pt(NH_3)_4]^{2+}\} + 28CO + 10H_2O \rightarrow \{[Pt_3(CO)_6]_3{}^{2-}\} + 20\{NH_4{}^{+}\} + 16NH_3 + 10CO_2 \quad (4)$$

The only unambiguous conclusion which can be drawn from the TPD of ammonia (Fig. 2) concerns thus the temperature shift of maxima evolution from the region 290–350°C for the Pt tetrammine ions to substantially lower temperature of the carbonylated samples (150–250°C). These latter maxima coincide with those from NH_4 zeolites without platinum.

The ratios of IR bands of integrated N–H vibrations in Pt tetrammine ions and in ammonia ions (Table 2) show higher absorption coefficient for the latter complexes. Considering, e.g. Eq. (3), the ratio of NH_3 in tetrammine ions to $NH_4{}^{+}$ formed is 24/14 (1.7); the experimental ratio is within 0.6–1.1, i.e. the absorption coefficient of $NH_4{}^{+}$ ions is in average twice larger.

4.4. Recarbonylation following removal of the CO ligands by mild oxidation and by 'low' temperature vacuum treatment in carbonyls synthesised from Pt tetrammines

The position of IR bands as well as the colour of carbonyls remain the same after oxidative removal of CO ligands within 25–150°C (see Fig. 4). The mechanism of this process was suggested in [8] assuming the exchange of CO ligands for oxygen and ammonia.

$$\{[Pt_3(CO_6)]_2{}^{2-}\} + \{14NH_4{}^{+}\} + 9O_2 \rightarrow \{[Pt_3O_3(NH_3)_3]_2\} + \{12H^{+}\} + H_2 + 8NH_3 + 12CO_2 \quad (5)$$

It follows from Fig. 5 that a majority of HF OH groups interacts with ammonia; they become free by vacuum treatment at 150°C (right-hand side) and also after following carbonylation (dotted spectrum, left-hand side). The upward shift of the positions of CO bands in recarbonylated samples after vacuum treatment (Fig. 4, dotted spectra) can be due either to the formation of carbonyls of higher nuclearity, or to another character of Pt carbonyls (neutral complexes?). The unchanged zeolitic matrix (Si/Al ratio, cavity dimensions) does not agree with the former possibility. The formation of a neutral carbonyl is supported by Longoni's linear dependency of on-top CO frequencies on the charge of the carbonyl [21,22]. The effect of vacuum decomposition of Pt anionic carbonyls on the recarbonylation will be discussed in more detail elsewhere.

5. Conclusions

It can be concluded that the high basicity of zeolitic oxygens in X and LSX zeolites stabilises the hexanuclear Pt anionic complexes ($[Pt_3(CO)_6]_2{}^{2-}$) regardless the platinum loading (examined between 3 and 18 wt.% of platinum). The increased Si/Al ratio (decreased basicity of zeolitic oxygens) results in the formation of a mixture of hexa and ennea nuclear complexes in Y zeolites reflected in a slight upward shift of positions of CO bands in the IR spectra; this shift does not depend on partial decationation of the zeolite. Higher Si/Al ratios in dealuminated Y and in EMT zeolite shift the IR bands to even higher wavenumbers, the highest shift occurs for Pt carbonyls on NaBEA, NaM and MCM-41 samples. The IR data point to the formation of Pt anionic carbonyls of higher nuclearity.The Si/Al ratio of the zeolites, reflected in the basicity of the zeolitic oxygens, thus seems to be the major factor affecting the nuclearity of Pt anionic carbonyls formed by the carbonylation of Pt^{2+} (in this case of parent Pt tetrammine ions or carbonyls decomposed in oxidising medium); low basicity of silicalites does not allow this process. The arrangement of the zeolite structure also plays an additional role, leading to pure triple stacked complexes in EMT and a mixture of double and triple stacked complexes in dealuminated Y with similar Si/Al ratio.

The carbonylation of Pt clusters formed by the decomposition of Pt anionic carbonyls in vacuum shifts the IR wavenumbers of CO ligands to higher wavenumbers regardless the unchanged Si/Al ratio of the zeolites. This is tentatively explained by the formation of neutral Pt carbonyl complexes.

Acknowledgements

This study was supported by the Grant Agency of the Academy of Sciences of the Czech Republic

(No. A4040710). The author thanks Mrs. Vašáková for measuring of the IR spectra.

References

[1] B.C. Gates, Chem. Rev. 95 (1995) 511.
[2] T. Yamamoto, T. Shido, S. Inagaki, Y. Fukushima, M. Ichikawa, J. Phys. Chem. B 102 (1998) 3866.
[3] M. Sasaki, M. Osada, N. Higashimoto, T. Yamamoto, A. Fukuoka, M. Ichikawa, J. Mol. Catal. A: Chem. 141 (1999) 223.
[4] D. Ozkaya, W. Zhou, J.M. Thomas, P. Midgley, V.J. Keast, S. Hermans, Catal. Lett. 60 (1999) 113.
[5] L. Kubelková, J. Vylita, L. Brabec, L. Drozdová, T. Bolom, J. Nováková, G. Schulz-Ekloff, N.I. Jaeger, J. Chem. Soc., Faraday Trans. I 92 (1996) 2035.
[6] L. Kubelková, L. Drozdová, L. Brabec, J. Nováková, J. Kotrla, P. Hülstede, N.I. Jaeger, G. Schulz-Ekloff, J. Phys. Chem. 100 (1996) 15517.
[7] M. Beneke, L. Brabec, J. Nováková, N. Jaeger, G. Schulz-Ekloff, J. Mol. Catal. A: Chem. 157 (2000) 151.
[8] Z. Bastl, M. Beneke, L. Brabec, P. Hülstede, N.I. Jaeger, J. Nováková, G. Schulz-Ekloff, Phys. Chem. Chem. Phys. 2 (2000) 3099.
[9] L. Kubelková, V. Seidl, J. Nováková, S. Bednárová, P. Jírû, J. Chem. Soc., Faraday Trans. I 80 (1984) 1367.
[10] L. Drozdová, L. Brabec, J. Nováková, M. Beneke, N. Jaeger, G. Schulz-Ekloff, Microporous Mesoporous Mater. 35/36 (2000) 511.
[11] I.V. Mishin, H. Bremer, K.P. Wendlandt, in: D. Kalló, Kh.M. Minachev (Eds.), Catalysis on Zeolites, Akadémiai Kiadó Budapest, 1988, p. 232.
[12] J.B. Higgins, R.B. LaPierre, J.L. Schlenker, A.C. Rohrman, J.D. Wood, G.T. Kerr, W.J. Rohrbaugh, Zeolites 8 (1988) 446.
[13] A. Ortlam, J. Rathouský, G. Schulz-Ekloff, A. Zukal, Microporous Mater. 6 (1996) 171.
[14] V. Bosáček, R. Klik, F. Genoni, G. Spano, F. Rivetti, F. Figueras, Magn. Reson. Chem. 37 (1999) S135.
[15] P.A. Jacobs, Carboniogenic Activity of Zeolites, Elsevier, Amsterdam, 1977, p. 48.
[16] L. Bengtsson-Kloo, C.M. Iapalucci, G. Longoni, S. Ulvenlund, Inorg. Chem. 37 (1998) 4355.
[17] J.C. Calabrese, L.F. Dahl, P. Chini, G. Longoni, S. Martinengo, J. Am. Chem. Soc. 96 (1974) 2614.
[18] D. Exner, N.I. Jaeger, K. Möller, G. Schulz-Ekloff, J. Chem. Soc., Faraday Trans. I (1982) 3537.
[19] G. Schulz-Ekloff, N.I. Jaeger, Catal. Today 3 (1988) 459.
[20] J. Nováková, L. Kubelková, L. Brabec, Z. Bastl, N. Jaeger, G. Schulz-Ekloff, Zeolites 16 (1996) 173.
[21] P. Chini, Rev. Inorg. Chem. Acta (1968) 3814.
[22] J.D. Roth, G.J. Lewis, L.K. Safford, X. Jiang, L.F. Dahl, M.J. Weaver, J. Am. Chem. Soc. 114 (1992) 6159.